Barrier distribution for the weakly bound stable projectile ^{7}Li with the medium-mass target nucleus ^{64}Ni

Md. Moin Shaikh,[1,*] Subinit Roy,[2] A. Mukherjee,[2] A. Goswami,[2,†] Balaram Dey,[3,‡]
S. Pal,[3] S. Roy,[3,§] A. Shrivastava,[4] S. K. Pandit,[4] and K. Mahata[4]

[1]*Department of Physics, Chanchal College, Chanchal, Malda, West Bengal 732123, India*
[2]*Saha Institute of Nuclear Physics, 1/AF, Bidhan Nagar, Kolkata 700064, India*
[3]*Tata Institute of Fundamental Research, Mumbai 400 005, India*
[4]*Nuclear Physics Division, Bhabha Atomic Research Centre, Mumbai 400 085, India*

Barrier distributions derived from fusion and back-angle quasielastic scattering excitation functions are important tools in understanding the reaction mechanisms in nucleus-nucleus collision at near-barrier energies. The excitation functions for the quasielastic scattering of ^{7}Li from the medium-mass target ^{64}Ni are measured at the angles $150°$ and $170°$ for the energy range of 12 to 24 MeV. The corresponding quasielastic barrier distribution function for this system is derived. The extracted barrier distribution is then compared with the previously measured fusion barrier distribution for the same system to look for any shift in the peak location to below-barrier energy as observed for the ^{6}Li + ^{64}Ni system. Further, the barrier distributions of the system ^{7}Li + ^{64}Ni from complementary measurements of the fusion and back-angle excitation functions are compared with the barrier distribution functions of ^{6}Li + ^{64}Ni. While ^{6}Li behaves like a weakly bound projectile, another stable isotope of Li, ^{7}Li, behaves more like a strongly bound projectile in collision with the same medium-mass target ^{64}Ni.

I. INTRODUCTION

Fusion is the most dominant reaction process near the Coulomb barrier energies. In heavy-ion collisions, the probability of fusion is further enhanced due to coupling of the relative motion in the entrance channel to other reaction degrees of freedom [1–7]. The evidence of channel coupling is also present in observables like the excitation functions and the near-barrier energy dependence of the interaction potential.

One major outcome of channel coupling is the splitting of the nominal Coulomb barrier of the colliding system into multiple barriers having varied degrees of penetrability associated with each of them. As a result, the function describing the distribution of these effective barriers or the barrier distribution (BD) becomes one of the powerful observables to understand the effect of channel coupling at near-barrier energies. The barrier distribution extracted from the precisely measured fusion excitation function, D_{fus}, provides a clearer signature of the effects modifying the fusion process at low energies [8,9].

A similar distribution of barriers can also be extracted from the back-angle quasielastic excitation function [10–12] as a consequence of the conservation of flux. But the BD derived from the back-angle quasielastic excitation function, D_{qel}, as argued by Zagrebaev [13], gives the distribution of the reaction thresholds. For collisions involving only strongly bound systems both these distributions demonstrate identical behavior [14] unless the reactants are very heavy. Barrier distributions, D_{fus} and D_{qel}, have been extracted for a large number of tightly bound systems [9,15–18]. It is observed that these complementary techniques yield BDs exhibiting behavior similar to that of the major peak at the Coulomb barrier energy, indicating that the barrier is the primary reaction threshold at low energies. A deviation is expected for collisions where nonfusion reaction channels present with a cross section comparable to the fusion cross section [19,20].

On the other hand, D_{fus} and D_{qel} have also been compared for a few systems involving weakly bound nuclei. The observations are quite different from those for strongly bound systems [21–23]. With weakly bound systems, the BDs are found to be wider, extending largely to subbarrier energies, and in many cases D_{fus} and D_{qel} do not peak at the same energy [24–29]. Lin *et al.* [26] observed that for weakly bound systems ^{6,7}Li + ^{208}Pb, ^{209}Bi there is a strong shift in the peak of D_{qel} to a lower energy compared to D_{fus}, but for the system ^{16}O + ^{144}Sm, where both the reaction partners are strongly bound, there is no significant difference between D_{fus} and D_{qel}. Palshetkar *et al.* [27] extracted D_{fus} and D_{qel} for the ^{6}Li + ^{197}Au system and reported a shift of the centroid

———————
*md.moinshaikh1987@gmail.com
†Deceased.
‡Present address: Bankura University, Purandarpur, Bankura, West Bengal 722155, India.
§Present address: Inter-University Centre for Astronomy and Astrophysics, Post Bag 4, Ganeshkhind, Pune, Maharashtra 411007, India.

of D_{qel} towards an energy lower by 3 MeV compared to the centroid of D_{fus}. The shift for the medium-heavy target ^{144}Sm with the same ^{6}Li projectile is about 1.5 MeV [28]. Jia *et al.* [29] compared D_{fus} and D_{qel} for the system ^{9}Be + ^{208}Pb and observed that the BDs match quite nicely with one another only when D_{qel} is shifted towards an energy higher by 1.5 MeV. In a previous work by our group [30,31], we demonstrated that for the ^{6}Li + ^{64}Ni system the D_{qel} peaked at an energy 450 keV lower compared to the peak of D_{fus}.

A systematic analysis of the observations with weakly bound projectiles indicates that the breakup degree of freedom broadens the BDs to subbarrier energies with the breakup-related nonfusion channel dominating over fusion. At the same time there is a shift in the peak locations of D_{qel} and D_{fus} and the shift depends upon the target mass as well as the breakup threshold of the projectile.

To further test the conjecture, we present in this article our study of D_{fus} and D_{qel} of the system ^{7}Li + ^{64}Ni and their comparison with the system ^{6}Li + ^{64}Ni. The back-angle quasielastic excitation function has been measured (Sec. II) to extract D_{qel} and compare it with D_{fus} from the previously measured fusion excitation function for the same system [32]. The primary motivation of this work is to see whether ^{7}Li ($S_\alpha = 2.47$ MeV) behaves like a weakly bound projectile such as ^{6}Li ($S_\alpha = 1.47$ MeV) with the same lower-medium-mass target nucleus ^{64}Ni.

II. EXPERIMENTAL DETAILS

The experiment was carried out in the General Purpose Scattering Chamber (GPSC) at the BARC-TIFR Pelletron Linac Facility in TIFR, Mumbai, India. A self-supporting $\approx 99\%$ enriched ^{64}Ni foil of thickness 507 ± 10 μg/cm^2, prepared by Oak Ridge National Laboratory, USA, was used as the target. The incident energy of the ^{7}Li beam was varied from 12 to 24 MeV and the Coulomb barrier of the ^{7}Li + ^{64}Ni system is close to 13.7 MeV in the laboratory. The energy was changed in small steps with a step size of 2 MeV for the energy range 24–20 MeV, 1 MeV for 20–15 MeV, and 0.5 MeV for the rest of the energy range. The beam current during the experiment was maintained in the range of 1 to 7 pnA. The outgoing backscattered particles were detected using two ΔE-E telescopes consisting of conventional silicon surface barrier detectors placed at $\theta_{lab} = \pm 170°$ with respect to the beam direction. Both the telescopes had 15-μm-thick ΔE detectors which were followed by 300-μm- and 1-mm-thick E detectors, respectively. The solid angle subtended by each telescope at the target center was estimated to be around 1.22 msr. A silicon surface barrier detector of thickness 2 mm was positioned at 150° with respect to the beam direction to achieve the required comparison with the previously reported quasielastic excitation function measurement for the system ^{6}Li + ^{64}Ni [31]. The solid angle of the single detector at the backward angle was 0.62 msr. In addition, two more single surface barrier detectors of thickness 500 μm and 3 mm, respectively, were positioned at $\pm 20°$ about the beam axis to monitor the beam position during the experiment. These detectors were also used for the purpose of normalization and target thickness verification. After each energy change,
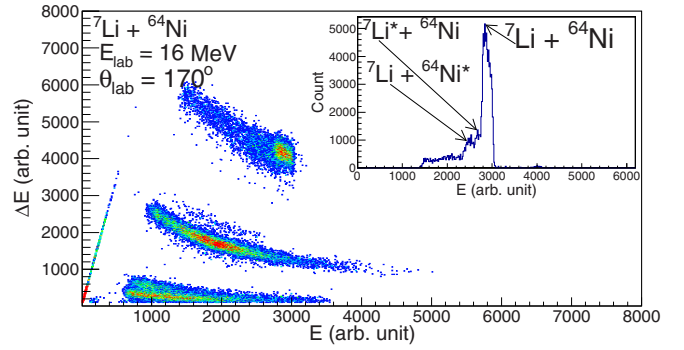

FIG. 1. A representative two-dimensional ΔE-E spectrum from the telescope at 170° for the system ^{7}Li + ^{64}Ni at a beam energy of 16 MeV. Inset: Energy projection of the elastic band. The elastically and inelastically scattered peaks are also marked.

calibration runs were taken using a standard ^{197}Au target. The events were recorded in the data acquisition system LAMPS [33] and an off-line version of the same was used to perform the data analysis. A representative two-dimensional plot at incident energy 16 MeV for the angle 170° showing the populated particle channels is presented in Fig. 1. The spectrum indicates that events corresponding to $Z = 1, 2,$ and 3 are clearly separated from one another. An energy projection of the elastic band is also shown in the inset in Fig. 1 and it is observed that the inelastically scattered events can be separated from elastic scattering. Peak positions corresponding to the elastic scattering and inelastic excitations to the first excited state of the projectile ^{7}Li* (0.478 MeV) and first excited state of the target ^{64}Ni* (1.345 MeV) are marked in the figure.

III. ANALYSIS AND RESULTS

A. Quasielastic scattering excitation function and corresponding barrier distribution D_{qel}

In the present work, the quasielastic scattering cross section is taken as the sum of cross sections of elastic and inelastic excitations of the projectile and the target. The quasielastic excitation functions have been measured by telescopes at $\pm 170°$ (equivalent angle with respect to the center-of-mass frame, $\theta_{c.m.} = \pm 171°$) and a single detector placed at 150° ($\theta_{c.m.} = 153°$).

The barrier distribution, D_{qel}, at a particular energy, is defined as the energy derivative of the ratio of the back-angle (180°) quasielastic differential cross section $d\sigma_{qel}$ to the Rutherford scattering differential cross section $d\sigma_R$ at the same angle [11],

$$D_{qel}(E) = -\frac{d}{dE}\left(\frac{d\sigma_{qel}}{d\sigma_R}\right), \quad (1)$$

and can be derived numerically using the point difference formula. As the measurement is performed at an angle $\theta_{c.m.}$ less than 180° for center-of-mass energy $E_{c.m.}$, a *centrifugal*
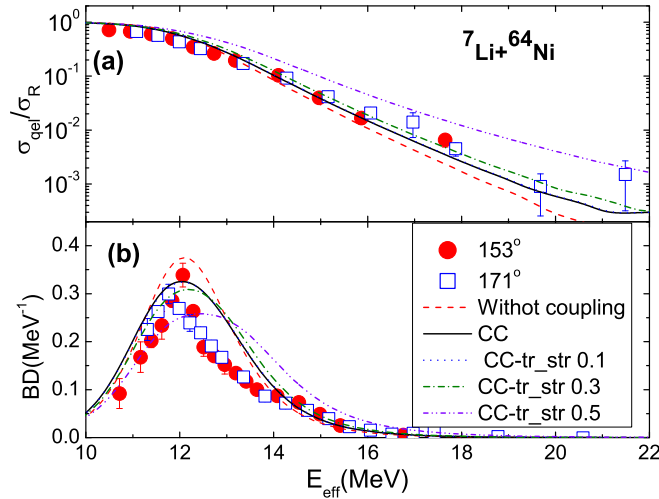
FIG. 2. Experimental (a) ratio to the Rutherford back-angle quasielastic scattering excitation function and (b) barrier distribution in comparison with the theoretical predictions. Filled circles and open squares represent the data corresponding to the angle $\theta_{c.m.} = 153°$ and $\theta_{c.m.} = 171°$, respectively, for the system $^7Li + ^{64}Ni$. The dashed line represents the calculation without the coupling condition; the solid line, the same with the coupling condition. Dotted, dashed-dotted, and dashed–double-dotted lines represent the effect of pair transfer coupling with coupling strengths 0.1, 0.3, and 0.5, respectively.
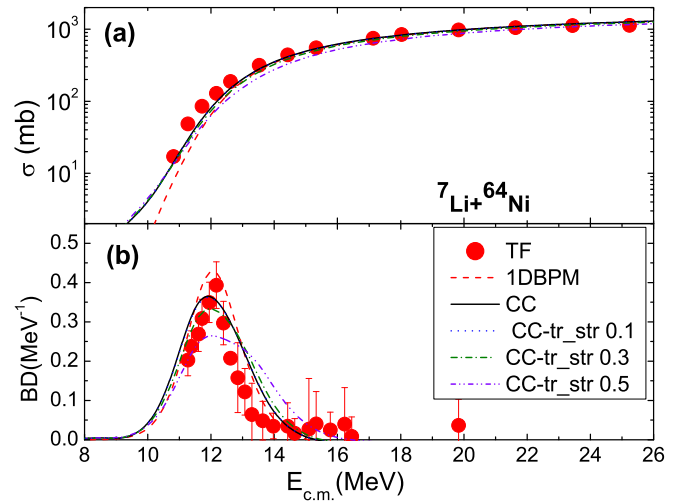

FIG. 3. (a) The experimental total fusion (TF) excitation function (solid bullets) in comparison with the one-dimensional barrier penetration model (1DBPM) and coupled-channel (CC) model predictions. (b) Barrier distribution (BD) functions derived from fusion excitation functions plotted in (a). Dashed and solid lines represent the calculated 1DBPM and CC predictions, respectively. Dotted, dashed-dotted, and dashed–double-dotted lines represent the effect of pair transfer coupling at coupling strengths 0.1, 0.3, and 0.5, respectively.

correction is needed to estimate the effective energy, E_{eff}, as

$$E_{eff} = E_{c.m.} \frac{2}{\text{cosec}(\theta_{c.m.}/2) + 1} \quad (2)$$

to obtain the equivalent cross section at 180°. The measured ratios of quasielastic cross sections to Rutherford cross sections at $\theta_{c.m.} = 171°$ ($\theta_{lab} = 170°$) and $\theta_{c.m.} = 153°$ ($\theta_{lab} = 150°$) as a function of the energy with centrifugal correction and correction for target thickness have been plotted in Fig. 2(a). The barrier distributions $D_{qel}(E)$ are extracted, using Eq. (1), from the quasielastic excitation functions for these angles and are shown in Fig 2(b). The filled circles represent the data corresponding to the angle $\theta_{c.m.} = 153°$ and the open squares represent the same for the angle $\theta_{c.m.} = 171°$, respectively. It is observed that the quasielastic barrier distributions obtained from the cross-section data for both angles are consistent with each other [34].

B. Fusion barrier distribution D_{fus} and comparison with D_{qel}

The barrier distribution $D_{fus}(E)$ has also been extracted from the previously measured total fusion excitation function for the system $^7Li + ^{64}Ni$ [32]. The excitation function and the extracted barrier distribution function are plotted in Figs. 3(a) and 3(b), respectively. The barrier distribution functions derived from the fusion and the back-angle quasielastic excitation functions are compared in Fig. 4. Conservation of flux in nuclear collision ensures that for light-ion-induced processes the complementary measurements of fusion and the back-angle quasielastic excitation functions yield similar barrier distribution functions with peaks at energies near the

Coulomb barrier of the system. However, for loosely bound light projectiles on heavy targets, due to the probability of breakup, deviations from the above picture have been observed. It is clear in Fig. 4 that for the $^7Li + ^{64}Ni$ system both the experimental barrier distributions peaked at almost
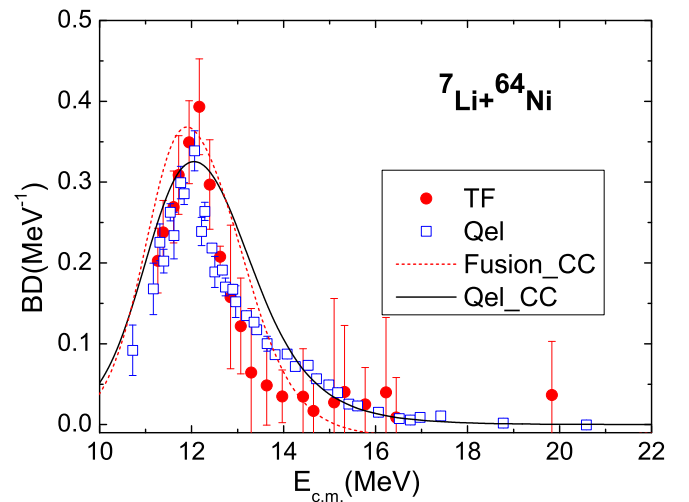

FIG. 4. Barrier distribution (BD) extracted from back-angle quasielastic excitation function in comparison with the same extracted from the fusion excitation function for the system $^7Li + ^{64}Ni$. Open squares and filled circles represent the BDs extracted from the quasielastic scattering and fusion excitation functions, respectively. Solid and dotted lines represent the BDs extracted from quasielastic scattering and fusion calculated from the coupled-channel calculation with the coupling condition.

TABLE I. Input real and imaginary potential parameters for CCQEL calculation.

			Potential		
V_0 (MeV)	r_0 (fm)	a (fm)	W_0 (MeV)	r_w (fm)	a_w (fm)
42.1	1.17	0.606	50.0	1.0	0.4

the same energy and their behaviors also match each other within the experimental uncertainties. This is contrary to the observation for the ^{6}Li + ^{64}Ni system [31].

IV. MODELING THE BARRIER DISTRIBUTIONS

As the complementary measurements of the barrier distribution yield the same distribution function for ^{7}Li + ^{64}Ni, we intend to perform the coupled-channel (CC) calculation for both the fusion and the back-angle quasielastic excitation functions. To explain the experimental observations, the model calculations have been carried out using the code CCQEL [35]. The reason for using the code is to find the simultaneous effect of channel coupling on the fusion and quasielastic scattering excitation functions and, hence, the BDs.

A complex nuclear potential has been used in the calculation, where the real part of the nuclear potential is the Akyüz-Winther potential [36] with the Woods-Saxon parametrization form. The imaginary part of the potential, on the other hand, also has the Woods-Saxon shape but the parameters are chosen such that the component simulates the ingoing-wave boundary condition for core fusion only. The potential parameters are listed in Table I. The corresponding parameters of the uncoupled barrier coming from the calculation with the chosen potential are the barrier height $V_B = 12.20$ MeV, the barrier radius $R_B = 9.25$ fm, and the barrier width $\hbar\omega = 3.56$ MeV, respectively.

In the coupling scheme of the CC calculation, inelastic excitations of both the projectile and the target have been introduced, taking the first excited states of the two colliding particles with the corresponding deformation parameters. A deformation parameter obtained from $B(E2) \uparrow = 7.59 e^2 \cdot$ fm^4 [37] has been used for the first excited state of ^{7}Li with $J^\pi = 1/2^-$ and $E^* = 0.478$ MeV. In the case of the target ^{64}Ni, a quadrupole deformation parameter $\beta_2 = 0.169$ [38] is used for the first excited state at $E^* = 1.345$ MeV and $J^\pi = 2^+$.

The effect of inelastic channel coupling on the back-angle quasielastic excitation function and the barrier distribution extracted from it is shown Fig. 2. The solid and dashed lines represent the theoretical predictions of the observables with and without inelastic coupling conditions, respectively. It is shown in Fig. 2(a) that the effect of inelastic channel coupling dominates the above-barrier energy region of the quasielastic scattering excitation function. Because of the coupling, the theoretical quasielastic cross sections have increased and come closer to the experimental data in the above-barrier energy region. But in the below-barrier region, as expected, the channel coupling does not show any cognizable effect.

The description of the quasielastic barrier distribution is also improved with the inelastic channel coupling. The CC calculation describes the experimental peak position of the barrier quite nicely, though the reproduction of the shape of the distribution is not very satisfactory. Figure 2 clearly indicates the requirement for other reaction channels in the description of the experimental data.

In a simultaneous analysis, the effect of channel coupling on fusion and the corresponding barrier distribution is shown in Fig. 3. The fusion cross sections in the no-coupling condition are used as the one-dimensional barrier penetration model (1DBPM) cross sections, which are represented by the dashed line, whereas solid lines represent the outcome of the CC calculation. It is shown in Fig. 3 that (a) channel coupling enhances the fusion cross sections at the subbarrier energy region but it does not have a significant effect at the above-barrier energies, and (b) the channel coupling affects only the peak height of the calculated barrier distribution. Both the model calculations reproduce the features of the experimental barrier distribution extracted from the fusion excitation function. Coupling to the inelastic states of the target and projectile does not have any strong effect on D_{fus} for the system ^{7}Li + ^{64}Ni.

To look for the effect of transfer coupling in a simultaneous calculation using the code CCQEL, we considered the coupling to $2n$ and d pair transfer channels. Both these two-particle transfer channels have low positive Q values, *viz.,* 2.14 and 2.83 MeV, respectively, for the ^{7}Li + ^{64}Ni system. It is not possible to distinguish between different combinations of pair transfer, i.e., between $2n$, $2p$, and d transfers in this code. These channels can only be separated by their Q values and the strengths of coupling, which is a parameter related to the transfer probability. As the transfer probability is still to be evaluated for these channels, the coupling strength is a free parameter in this system. However, the coupling strength can be constrained in the present work through a simultaneous reproduction of the complementary reaction observables, the quasielastic scattering and fusion excitation functions, and the secondary observables, the distribution of barriers.

It is found from the calculation that the small difference in Q values of the two channels does not have any significant effect in altering the excitation functions. Hence, the transfer coupling calculations have been performed with different values for the coupling strengths with an average of the Q values of these two channels. The effect of transfer coupling on quasielastic scattering and fusion is depicted in Figs. 2 and 3 using dotted, dashed-dotted, and dashed–double-dotted lines for coupling strengths of 0.1, 0.3, and 0.5, respectively. It is observed from both figures that a coupling strength of 0.1 does not have any significant effect on the quasielastic scattering or fusion excitation functions or the barrier distributions obtained from these excitation functions. When the strength is increased to 0.3 the reproduction of quasielastic scattering excitation improves slightly on the higher-energy side but an indication of mismatch is observed on the lower-energy side for both the quasielastic scattering and the fusion excitation functions. These figures also show that the coupling strength cannot be as large as 0.5 because for this strength value the mismatch with the data is too great for all the reaction
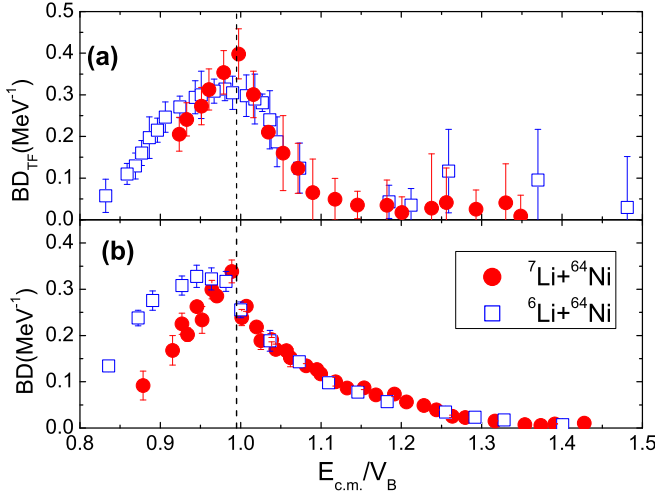
FIG. 5. Comparison of BDs extracted from (a) fusion and (b) back-angle quasielastic excitation functions for the systems $^7\text{Li} + ^{64}\text{Ni}$ (filled circles) and $^6\text{Li} + ^{64}\text{Ni}$ (open squares). The vertical dashed line indicates the peak position of the BDs for the system $^7\text{Li} + ^{64}\text{Ni}$, which matches the peak position of the fusion BDs for the system $^6\text{Li} + ^{64}\text{Ni}$.

observables. From Figs. 2 and 3 one may infer that pair transfer coupling can have some effect on reaction observables for the system $^7\text{Li} + ^{64}\text{Ni}$ and the upper limit of the strength of that coupling can be 0.3. But this coupling is very weak and it does not play any significant role in the reaction mechanism for this system.

The BDs derived from the fusion and the back-angle quasielastic excitation are compared in Fig. 4. It is clearly observed that both experimental distributions for the $^7\text{Li} + ^{64}\text{Ni}$ system peaked at almost the same energy and their behaviors also match each other within the experimental uncertainties. The theoretical barrier distributions, obtained from CC calculations, also exhibit the same behavior. According to Zagrebaev [13] the quasielastic barrier distribution actually gives the distribution of reaction thresholds rather than the potential barrier distribution and the two give the same distribution when fusion completely dominates the reaction cross section at low energies, a feature associated with strongly bound systems. Thus the primary observation in the present work indicates that the effect of any other direct reaction channels on the reaction cross section for the $^7\text{Li} + ^{64}\text{Ni}$ system is not as significant as fusion at low energies and ^7Li behaves like a strongly bound projectile against the target ^{64}Ni.

V. COMPARISON WITH $^6\text{Li} + ^{64}\text{Ni}$

In this section, the nature of the barrier distributions derived from two complementary measurements for the system $^7\text{Li} + ^{64}\text{Ni}$ are compared with the previously reported results for the $^6\text{Li} + ^{64}\text{Ni}$ system [31]. Figure 5 depicts a comparison of the BDs from the fusion [Fig. 5(a)] as well as from the back-angle quasielastic [Fig. 5(b)] excitation functions for the two systems.

It is observed that the barrier distributions obtained from the fusion excitation functions for both the systems peaked

almost at the Coulomb barrier energy of the respective system. However, the fusion barrier distribution of $^6\text{Li} + ^{64}\text{Ni}$ has a comparatively wider shape.

But a distinct difference in barrier distributions from the quasielastic excitation functions for $^7\text{Li} + ^{64}\text{Ni}$ and $^6\text{Li} + ^{64}\text{Ni}$ is clearly visible. In the above-barrier energy region both the barrier distributions show a similar behavior. While the BD from the back-angle quasielastic excitation function for the $^7\text{Li} + ^{64}\text{Ni}$ system peaked at the barrier energy, the distribution for the system $^6\text{Li} + ^{64}\text{Ni}$ peaked at an energy roughly about 450 keV [31] lower than the barrier energy. Also, the distribution function for the case of the $^6\text{Li} + ^{64}\text{Ni}$ system extends significantly to the below-barrier energy side, generating a much wider BD compared to that for the $^7\text{Li} + ^{64}\text{Ni}$ system. The observation indicates that the reaction threshold for the more weakly bound system $^6\text{Li} + ^{64}\text{Ni}$ is shifted towards lower energies compared to the system $^7\text{Li} + ^{64}\text{Ni}$, although the two-body breakup threshold of the latter is only about a MeV higher.

The comparison of barrier distributions from the fusion and back-angle quasielastic excitation functions signifies that for the $^7\text{Li} + ^{64}\text{Ni}$ system the fusion and reaction barriers are the same, but for $^6\text{Li} + ^{64}\text{Ni}$ the reaction barrier is lower than the fusion barrier. Thus in a collision with the light-medium-mass target ^{64}Ni, although the projectile ^7Li behaves more like a strongly bound system, for its weakly bound partner ^6Li, with a two-body breakup threshold of 1.47 MeV, nonfusion reaction channels are still open below the barrier energy.

The observation of the present work conforms with the trend in the experimental results from the collision of Li isotopes with targets of different masses. Both the isotopes behave as weakly bound systems, with regard to the width and energy shift in peak locations of the BDs from two complementary sources, for heavy targets. With a decreasing target mass, ^7Li starts behaving like a strongly bound projectile well before its stable isotopic partner ^6Li. For the ^6Li projectile, while the energy shift in the peak location of the BDs decreases with a decreasing charge product of the colliding nuclei and becomes negligibly small for light targets, the width of the distribution function remains wide, extending to below-barrier energies even for a light-mass target like ^{28}Si [23–25].

VI. SUMMARY

Measurement of back-angle quasielastic scattering excitation functions has been performed at $\theta_{\text{lab}} = 150°$ and $\theta_{\text{lab}} = 170°$ for the system $^7\text{Li} + ^{64}\text{Ni}$ at near-barrier energies. Barrier distributions are extracted from the measured excitation functions and both of them show a similar distribution pattern. The BD has also been extracted from previously measured fusion excitation functions for $^7\text{Li} + ^{64}\text{Ni}$. The resultant BDs from fusion and quasielastic scattering have been compared and it is found that both distributions show almost the same behavior, peaking at the Coulomb barrier energy and having almost the same width. Since in the present study no significant difference between the two is observed, i.e., the back-angle quasielastic BD representing the reaction threshold distribution is the same as the fusion BD, it can be concluded

that fusion is the most dominant reaction channel around the barrier energies for the system ^{7}Li + ^{64}Ni.

A coupled-channel calculation has been performed to understand the effect of channel coupling simultaneously on the quasielastic and fusion excitation functions and also on the corresponding extracted BDs. The description of the experimental observables has improved with the introduction of coupling of inelastic channels, but the improvement is not enough to exactly describe the experimental BDs, especially the widths, either for the fusion or for the quasielastic scattering cases. The same coupling predominantly affects the above-barrier energy region for fusion and the subbarrier region for quasielastic scattering. The calculation also indicates that pair transfer coupling does not have any significant effect on the reaction mechanism for the system of the current study.

The barrier distributions of the system ^{7}Li + ^{64}Ni are also compared with the barrier distributions of ^{6}Li + ^{64}Ni. The fusion BDs for both systems peak at the respective barrier energies, with relatively less bound ^{6}Li + ^{64}Ni having a slightly broader distribution. Again, in comparing the BDs from the back-angle quasielastic excitation functions, the observation of the BD for ^{6}Li + ^{64}Ni, extending significantly to subbarrier energies relative to ^{7}Li + ^{64}Ni, leads to the conclusion that the reaction threshold is different from the fusion one for the more weakly bound system ^{6}Li + ^{64}Ni. Therefore, in a collision with the light-medium-mass nucleus ^{64}Ni, even though ^{6}Li behaves as a weakly bound projectile, ^{7}Li, with a breakup threshold at 2.47-MeV excitation, acts more like a strongly bound projectile.

[1] S. G. Steadman and M. J. Rhoades-Brown, Annu. Rev. Nucl. Sci. **36**, 649 (1986).

[2] M. Beckerman, Rep. Prog. Phys. **51**, R1047 (1988).

[3] C. H. Dasso, S. Landowne, and A. Winther, Nucl. Phys. A **405**, 381 (1983); Nucl. Phys. **407**, 221 (1983).

[4] R. A. Broglia, C. H. Dasso, S. Landowne, and A. Winther, Phys. Rev. C **27**, 2433(R) (1983).

[5] G. R. Satchler, Phys. Rep. **199**, 147 (1991).

[6] B. B. Back, H. Esbensen, C. L. Jiang, and K. E. Rehm, Rev. Mod. Phys. **86**, 317 (2014).

[7] K. Hagino and N. Takigawa, Prog. Theor. Phys. **128**, 1061 (2012).

[8] N. Rowley, G. R. Satchler, and P. H. Stelson, Phys. Lett. B **254**, 25 (1991).

[9] M. Dasgupta, D. J. Hinde, N. Rowley, and A. M. Stefanini, Annu. Rev. Part. Sci. **48**, 401 (1998).

[10] A. B. Balantekin and P. E. Reimer, Phys. Rev. C **33**, 379 (1986).

[11] H. Timmers, J. R. Leigh, M. Dasgupta, D. J. Hinde, R. C. Lemmon, J. C. Mein, C. R. Morton, J. O. Newton, and N. Rowley, Nucl. Phys. A **584**, 190 (1995).

[12] K. Hagino and N. Rowley, Phys. Rev. C **69**, 054610 (2004).

[13] V. I. Zagrebaev, Phys. Rev. C **78**, 047602 (2008).

[14] H. Timmers, D. Ackermann, S. Beghini, L. Corradi, J. H. He, G. Montagnoli, F. Scarlassara, A. M. Stefanini, and N. Rowley, Nucl. Phys. A **633**, 421 (1998).

[15] H. Zhang, F. Yang, C. Lin, Z. Liu, and Y. Hu, Phys. Rev. C **57**, 1047(R) (1998).

[16] R. F. Simões, D. S. Monteiro, L. K. Ono, A. M. Jacob, J. M. B. Shorto, N. Added, and E. Crema, Phys. Lett. B **527**, 187 (2002).

[17] E. Piasecki, Ł. Świderski, N. Keeley, M. Kisielinski, M. Kowalczyk, S. Khlebnikov, T. Krogulski, K. Piasecki, G. Tiourin, M. Sillanpaa, W. H. Trzaska, and A. Trzcinska, Phys. Rev. C **85**, 054608 (2012).

[18] G. Kaur, B. R. Behera, A. Jhingan, B. K. Nayak, R. Dubey, P. Sharma, M. Thakur, R. Mahajan, N. Saneesh, T. Banerjee, Khushboo, A. Kumar, S. Mandal, A. Saxena, P. Sugathan, and N. Rowley, Phys. Rev. C **94**, 034613 (2016).

[19] S. Mitsuoka, H. Ikezoe, K. Nishio, K. Tsuruta, S. C. Jeong, and Y. Watanabe, Phys. Rev. Lett. **99**, 182701 (2007).

[20] S. S. Ntshangase, N. Rowley, R. A. Bark, S. V. Förtsch, J. J. Lawrie, E. A. Lawrie, R. Lindsay, M. Lipoglavsek, S. M. Maliage, L. J. Mudau, S. M. Mullins, O. M. Ndwandwe, R. Neveling, G. Sletten, F. D. Smit, and C. Theron, Phys. Lett. B **651**, 27 (2007).

[21] L. F. Canto, P. R. S. Gomes, R. Donangelo, and M. S. Hussein, Phys. Rep. **424**, 1 (2006).

[22] L. F. Canto, P. R. S. Gomes, R. Donangelo, J. Lubian, and M. S. Hussein, Phys. Rep. **596**, 1 (2015).

[23] K. Zerva, A. Pakou, N. Patronis, P. Figuera, A. Musumarra, A. Di Pietro, M. Fisichella, T. Glodariu, M. La Commara, M. Lattuada, M. Mazzocco, M. G. Pellegriti, D. Pierroutsakou, A. M. Sanchez-Benitez, V. Scuderi, E. Strano, and K. Rusek, Eur. J. Phys. A **48**, 102 (2012).

[24] K. Zerva, N. Patronis, A. Pakou, N. Alamanos, X. Aslanoglou, D. Filipescu, T. Glodariu, M. Kokkoris, M. La Commara, A. Lagoyannis, M. Mazzocco, N. G. Nicolis, D. Pierroutsakou, M. Romoli, and K. Rusek, Phys. Rev. C **80**, 017601 (2009).

[25] K. Zerva, A. Pakou, K. Rusek, N. Patronis, N. Alamanos, X. Aslanoglou, D. Filipescu, T. Glodariu, N. Keeley, M. Kokkoris, M. La Commara, A. Lagoyannis, M. Mazzocco, N. G. Nicolis, D. Pierroutsakou, and M. Romoli, Phys. Rev. C **82**, 044607 (2010).

[26] C. J. Lin, H. Q. Zhang, F. Yang, M. Ruan, Z. H. Liu, Y. W. Wu, X. K. Wu, P. Zhou, C. L. Zhang, G. L. Zhang, G. P. An, H. M. Jia, and X. X. Xu, Nucl. Phys. A **787**, 281 (2007).

[27] C. S. Palshetkar, S. Thakur, V. Nanal, A. Shrivastava, N. Dokania, V. Singh, V. V. Parkar, P. C. Rout, R. Palit, R. G. Pillay, S. Bhattacharyya, A. Chatterjee, S. Santra, K. Ramachandran, and N. L. Singh, Phys. Rev. C **89**, 024607 (2014).

[28] D. S. Monteiro, P. R. S. Gomes, and J. Lubian, Phys. Rev. C **80**, 047602 (2009).

[29] H. M. Jia, C. J. Lin, H. Q. Zhang, Z. H. Liu, N. Yu, F. Yang, F. Jia, X. X. Xu, Z. D. Wu, S. T. Zhang, and C. L. Bai, Phys. Rev. C **82**, 027602 (2010).

[30] Md. Moin Shaikh, Subinit Roy, S. Rajbanshi, M. K. Pradhan, A. Mukherjee, P. Basu, S. Pal, V. Nanal, R. G. Pillay, and A. Shrivastava, Phys. Rev. C **90**, 024615 (2014).

[31] Md. Moin Shaikh, Subinit Roy, S. Rajbanshi, M. K. Pradhan, A. Mukherjee, P. Basu, S. Pal, V. Nanal, R. G. Pillay, and A. Shrivastava, Phys. Rev. C **91**, 034615 (2015).

[32] Md. Moin Shaikh, Subinit Roy, S. Rajbanshi, A. Mukherjee, M. K. Pradhan, P. Basu, V. Nanal, S. Pal, A. Shrivastava, S. Saha, and R. G. Pillay, Phys. Rev. C **93**, 044616 (2016).

[33] Computer code LAMPS (Linux Advanced Multiparameter System), www.tifr.res.in/~pell/lamps.html.

[34] Md. Moin Shaikh, Subinit Roy, A. Mukherjee, A. Goswami, B. Dey, S. Pal, S. Roy, A. Shrivastava, S. K. Pandit, and K. Mahata, JPS Conf. Proc. **32**, 010035 (2020).

[35] K. Hagino, N. Rowley, and A. T. Kruppa, Comput. Phys. Commun. **123**, 143 (1999).

[36] O. Akyüz and A. Winther, in *Proceedings, International School of Physics Enrico Fermi, Course LXXVII*, edited by R. A. Broglia, R. A. Ricci, and C. H. Dasso (Noah-Holland, Amsterdam, 1981), p. 492.

[37] W. J. Vermeer, R. H. Spear, and F. C. Barker, Nucl. Phys. A **500**, 212 (1989).

[38] B. Pritychenko, M. Birch, B. Singh, and M. Horoi, At. Data Nucl. Data Tables **107**, 1 (2016).